WATER RESOURCES RESEARCH, VOL. 35, NO. 11, PAGES 3507–3521, NOVEMBER 1999

Effects of hydraulic roughness on surface textures of gravel-bed rivers

John M. Buffington[1] and David R. Montgomery
Department of Geological Sciences, University of Washington, Seattle

Abstract. Field studies of forest gravel-bed rivers in northwestern Washington and southeastern Alaska demonstrate that bed-surface grain size is responsive to hydraulic roughness caused by bank irregularities, bars, and wood debris. We evaluate textural response by comparing reach-average median grain size (D_{50}) to that predicted from the total bank-full boundary shear stress ($\tau_{0_{bf}}$), representing a hypothetical reference condition of low hydraulic roughness. For a given $\tau_{0_{bf}}$, channels with progressively greater hydraulic roughness have systematically finer bed surfaces, presumably due to reduced bed shear stress, resulting in lower channel competence and diminished bed load transport capacity, both of which promote textural fining. In channels with significant hydraulic roughness, observed values of D_{50} can be up to 90% smaller than those predicted from $\tau_{0_{bf}}$. We find that wood debris plays an important role at our study sites, not only providing hydraulic roughness but also influencing pool spacing, frequency of textural patches, and the amplitude and wavelength of bank and bar topography and their consequent roughness. Our observations also have biological implications. We find that textural fining due to hydraulic roughness can create usable salmonid spawning gravels in channels that otherwise would be too coarse.

1. Introduction

The surface grain size of gravel-bed rivers reflects the caliber and volume of sediment that is supplied to the channel, as well as the time-integrated frequency and magnitude of discharge events that are capable of moving sediment. Surface grains move when the bed shear stress (τ') exceeds the critical stress for grain motion (τ_c)

$$q_b = k(\tau' - \tau_c)^n \tag{1}$$

where q_b is the bed load transport capacity (i.e., the transport rate of a channel unlimited by sediment supply) and k and n are empirical values [*du Boys*, 1879; *O'Brien and Rindlaub*, 1934; *Meyer-Peter and Müller*, 1948; *Chien*, 1956; *Wathen et al*., 1995]. Here τ' is that portion of the total boundary shear stress that is applied to the bed and responsible for sediment transport. It is defined as the total boundary shear stress (τ_0) corrected for momentum losses caused by hydraulic roughness other than grain skin friction [*Einstein and Banks*, 1950; *Einstein and Barbarossa*, 1952; *Nelson and Smith*, 1989]

$$\tau' = \tau_0 - \tau'' - \tau''' - \cdots \tau^n \tag{2}$$

$$\text{bed} = \text{total} - \text{banks} - \text{bed forms} - \cdots \text{other}$$

The critical, grain-mobilizing shear stress for a grain size of interest (τ_{c_i}) is a function of submerged grain weight, particle protrusion into the flow, and intergranular friction angle [*Wiberg and Smith*, 1987; *Kirchner et al*., 1990; *Buffington et al*., 1992; *Johnston et al*., 1998]; the latter two depend on sediment sorting (σ) and the size of the particle of interest (D_i) relative to its neighbors (D_i/D_{50}, where D_{50} is the median bed-surface grain size) [*Kirchner et al*., 1990; *Buffington et al*., 1992; *Johnston et al*., 1998].

The broad grain-size distributions of gravel-bed rivers (typically sand to cobble) allow for considerable selective transport and dynamic textural response to local perturbations of sediment supply or transport capacity [*Dietrich et al*., 1989]. For example, a local transport capacity greater than supply may result in winnowing of fine grains and textural coarsening. Textural coarsening, in turn, creates a rougher surface with greater intergranular friction angles, increasing critical shear stresses for grains moving over the bed (τ_{c_i}) [*Kirchner et al*., 1990; *Buffington et al*., 1992; *Johnston et al*., 1998] thereby retarding bed load transport rates (equation (1)). Altered bed-surface roughness also affects local velocity structure and bed shear stress [*Naot*, 1984; *Wiberg and Smith*, 1991]. Consequently, there is a dynamic feedback between bed-surface texture, bed shear stress, and transport capacity. Given sufficient time, constancy of sediment and water inputs, and availability of mobile sediment, the above process feedbacks will ultimately result in equilibration of the transport rate with the imposed sediment supply rate [*Dietrich et al*., 1989; *Lisle et al*., 1993]. Selective transport that results in bed-surface coarsening and armor development also makes the bed surface less mobile and alters the timing and total contribution of subsurface sediment to the supply of bed load material [*Milhous*, 1973; *Parker and Klingeman*, 1982; *Carling and Hurley*, 1987].

In this paper we examine the effects of hydraulic roughness on bed-surface grain size in complex forest channels. Gravel-bed rivers in forested mountain drainage basins commonly contain numerous sources and scales of hydraulic roughness within a single reach, such as bed-surface skin friction; form drag due to bars and in-channel flow obstructions (boulders, wood debris, and bedrock projections); skin friction and form

[1]Now at Water Resources Division, U.S. Geological Survey, Boulder, Colorado.

Paper number 1999WR900138.
0043-1397/99/1999WR900138$09.00

drag caused by riparian vegetation lining the banks and protruding into the flow; and momentum losses due to downstream changes in channel width and planform curvature. These hydraulic roughness elements can significantly reduce the bed shear stress (equation (2)). For example, form drag due to bed forms in sand-bed and gravel-bed rivers can result in bed stresses that are 10–75% less than the total boundary shear stress [*Parker and Peterson*, 1980; *Prestegaard*, 1983; *Dietrich et al*., 1984; *Hey*, 1988].

We hypothesize that channels with greater hydraulic roughness will have smaller proportions of total boundary shear stress available for sediment transport (equation (2)) and thus will have decreased competence and finer bed surfaces. In this paper we develop a framework for examining grain-size response to hydraulic roughness and test the above hypothesis using field data from forest gravel-bed channels.

2. Analysis Framework

Our method for examining textural response to hydraulic roughness involves comparing observed bed-surface grain sizes to those predicted for a hypothetical, low-roughness reference state [*Dietrich et al*., 1996].

2.1. Reference State

In the absence of major hydraulic resistance the bed shear stress is approximately equal to the total boundary shear stress (equation (2)). This hypothetical, end-member condition of low hydraulic roughness is visualized as a wide, straight, planar channel with relatively small grain sizes that do not offer significant form drag. The competent, median, bed-surface grain size (D_{50}) for this channel can be predicted from the *Shields* [1936] equation, which is a force balance between the driving fluid stresses and the resisting grain weight per unit area at incipient particle motion

$$\tau^*_{c50} = \tau_{c50}/[D_{50}(\rho_s - \rho)g] \tag{3}$$

where ρ and ρ_s are the fluid and sediment densities (set equal to 1000 and 2650 kg/m^3, respectively), τ_{c50} and τ^*_{c50} are the dimensional and dimensionless critical shear stresses for incipient motion of D_{50}, respectively, and g is gravitational acceleration. We set τ^*_{c50} equal to 0.030, a conservative value for visually based methods of determining incipient motion and one which may minimize error caused by neglect of roughness elements [*Buffington and Montgomery*, 1997]. Rearranging the Shields equation allows determination of the competent median grain size for a given bed stress

$$D_{50} = \tau'/[\tau^*_{c50}(\rho_s - \rho)g] \tag{4}$$

where $\tau' \equiv \tau_{c50}$. We define τ_{c50} specifically as the bank-full bed stress (τ'_{bf}), which is approximately equal to the total bank-full boundary shear stress ($\tau_{0_{bf}}$) for our low-roughness reference channel. We choose bank-full flow as our reference condition because it is the practical limit of shear stress in natural channels with well-developed floodplains and self-formed beds (i.e., all sizes mobile at typical high flows). Furthermore, the bank-full flow is believed to be a morphologically significant discharge for gravel-bed rivers [*Wolman and Miller*, 1960; *Henderson*, 1963; *Li et al*., 1976; *Carling*, 1988], many of which exhibit a near-bank-full threshold for significant sediment transport [*Leopold et al*., 1964; *Parker*, 1978, 1979; *Howard*, 1980; *Anderews*, 1984].

The reference D_{50} is the limit of channel competence (maximum mobile D_{50}) for a river with vanishingly small hydraulic roughness other than grain skin friction (i.e., $\tau' \approx \tau_0$, see (2)). It is important to note, however, that the reference D_{50} is a hypothetical grain size, the actual occurrence of which depends on the volume and caliber of sediment supplied to the channel, which, in turn, is a basin-specific function of geology, geomorphic processes, and anthropogenic disturbance.

2.2. Hypothesis

On the basis of the above theory we hypothesize that channels with greater hydraulic roughness will have lower bed stresses (equation (2)) and therefore will have smaller bed-surface grain sizes than that predicted from the total boundary shear stress (i.e., (4) with $\tau' < \tau_0$ versus $\tau' = \tau_0$). Consequently, for a given total boundary shear stress we expect a systematic textural fining with increasing hydraulic roughness and lower bed stress. The magnitude of textural fining should reflect both the decrease in competence and the degree of fine-sediment deposition forced by hydraulic roughness and lower bed stresses. Hydraulic roughness that lowers τ' should decrease the bed load transport capacity (equation (1)), resulting in reduced bed-surface grain size due to deposition of fine-grained particles (those typically in transport and comprising the majority of the bed load). To examine the effects of hydraulic roughness on surface grain size, we predict competent median grain sizes for channels with low hydraulic roughness ((4), with $\tau' = \tau_0$) and compare these values to observed median grain sizes in channels with systematically greater hydraulic roughness.

2.3. Reach-Scale Approximation

Because flow perturbations caused by roughness elements are spatially complex and inherently nonlinear, we examine grain-size response to hydraulic roughness at reach scales, simplifying our analysis. Over sufficiently long reaches in channels with relatively slowly varying discharges, the reach-average total boundary shear stress can be approximated by a depth-slope product ($\tau_0 = \rho g h S$, where h and S are the reach-average channel depth and slope, respectively). Applying this approximation and remembering that $\tau_{c50} \equiv \tau'_{bf} \approx \tau_{0_{bf}}$ for our low-roughness reference channel, (4) is rewritten as

$$D_{50} = \frac{\rho g h S}{\tau^*_{c50}(\rho_s - \rho)g} \tag{5}$$

where h and S are reach-average bank-full values. We leave (5) unsimplified because our ultimate goal is to predict a reference D_{50} as a function of the bank-full shear stress. Use of the depth-slope product assumes steady, uniform flow. *Paola and Mohrig* [1996] argue that to assume quasi-steady flow, significant discharge fluctuations should occur on timescales $\gg u/gS$ (where u is the reach-average downstream velocity), while quasi-uniform flow requires study reach lengths $\gg h/S$. In hydraulically complex forest channels the depth-slope product is valid only as a reach-average approximation of the total boundary shear stress. Large, frequently spaced roughness elements cause locally nonuniform flow, making the depth-slope product inappropriate for subreach scales.

3. Study Sites and Methods

To examine textural response to hydraulic roughness, a field study of plane-bed channels (definition of *Montgomery and*

Buffington [1997]), wood-poor pool-riffle channels, and wood-rich pool-riffle channels was conducted in forest mountain drainage basins of northwestern Washington and southeastern Alaska (Figure 1). These three channel types represent a general cumulative addition of bank, bar, and wood-debris roughness and a progressive decrease in τ' for a given τ_0 (equation (2)).

3.1. Olympic Peninsula

We surveyed fourteen channels on the Olympic Peninsula of northwestern Washington. The Olympic Peninsula is characterized by mountainous terrain and a coastal rain forest of Sitka spruce (*Picea sitchensis*), western hemlock (*Tsuga heterophylla*), red cedar (*Thuja plicata*), and Douglas fir (*Pseudotsuga taxifolia*). Bedrock geology of the peninsula is predominantly composed of Eocene to Miocene marine basalts and sediments [*Tabor and Cady*, 1978a, b]. The Olympic study sites occupy watersheds influenced by Pleistocene glaciation and are typically incised into fluvioglacial deposits. Channel widths and slopes of our study sites ranged from 5 to 13 m and from 0.0040 to 0.0265, respectively (Table 1).

Logging activity on the Olympic Peninsula is generally intensive, with some forests on their third harvest rotation within the last 100 years. Most study sites had riparian buffers composed of mixed shrub and conifer, although some study sites had been clear cut to channel margins, resulting in riparian forests of mixed shrub and red alder (*Alnus rubra*). Coniferous buffers were typically second growth, indicating a long history of logging disturbance. Hillslope failures are common in the Olympic Peninsula, and relict debris-flow deposits form channel-margin terraces in three of the study reaches, indicating both long run-out paths and the potential for periodic large sediment inputs.

At each study site, three cross sections and a center-line bed profile were surveyed in reaches that were 8 to 18 channel widths long. Detailed topographic, textural, and wood maps also were constructed using a digital theodolite. Bed surfaces were commonly composed of spatially distinct textural patches (i.e., grain size facies) of differing particle size and sorting. A standard procedure was developed to classify textural patches [*Buffington and Montgomery*, 1999]. Surface grain sizes of each patch type were determined from random pebble counts [*Wolman*, 1954] of 100^+ grains. These samples were, in turn, spatially averaged by patch area to determine reach-average grain-size statistics. The lower limit of grain-size measurement was 2 mm, with smaller sizes grouped as a single category. We did not truncate data collection at the lower limit of grain-size measurement as is commonly recommended [*Kellerhals and Bray*, 1971; *Church et al*., 1987] because it can distort the size distribution. Particle sizes suspendable at bank-full stage were removed from the grain-size distributions to separate bed load from suspended load. The maximum suspendable size was calculated from *Dietrich*'s [1982] settling velocity curves, assuming a Corey shape factor of 0.7, a Power's roundness of 3.5, and a settling velocity equal to the bank-full shear velocity. Suspendable grain sizes ranged from 2 to 8 mm.

3.2. Southeastern Alaska

We supplemented our Olympic survey with data from 27, southeast Alaskan, coastal channels studied by *Wood-Smith and Buffington* [1996] (Table 1). The Alaskan study areas are characterized by steep glaciated terrain, maritime climate, and rain forests predominantly composed of Sitka spruce and western hemlock. Hillslopes are commonly grooved by avalanche

Figure 1. Photographs of (a) plane-bed, (b) wood-poor pool-riffle, and (c) wood-rich pool-riffle channels of northwestern Washington and southeastern Alaska.

Table 1a. Reach-Average Olympic Channel Characteristics

Channel	S	W, m	h,* m	L, m	D_{50},† mm	$\sigma_g(\phi)$†,‡	SE_{50},† mm	LWD Per Square Meter	$(\alpha/\lambda)_b$	$(\alpha/\lambda)_w$
Plane-Bed/Incipient Pool-Riffle										
Dry 2§	0.0126	6.84	0.59 (0.69)	60	67.1 (69.2)	1.24 (1.17)	0.0 (0.0)	0.0000	0.000	0.018
Alder‖	0.0265	8.68	0.57 (0.64)	154	52.8 (58.0)	1.60 (1.28)	5.9 (5.5)	0.0015	0.010	0.023
Hoko 2	0.0160	5.12	0.34 (0.37)	60	54.8 (55.2)	1.34 (1.31)	0.0 (0.0)	0.0033	0.008	0.024
Hoh 1	0.0059	11.53	0.55 (0.62)	142	19.3 (41.9)	2.17 (1.19)	8.3 (0.8)	0.0006	0.008	0.008
Hoh 2	0.0114	10.08	0.51 (0.55)	95	56.8 (62.1)	1.59 (1.48)	7.6 (2.5)	0.0052	0.010	
Wood-Poor Pool-Riffle										
Skunk 2	0.0126	6.79	0.83 (0.89)	85	39.3 (41.2)	1.11 (0.98)	9.1 (8.4)	0.0243	0.012	0.056
Hoko 1	0.0085	12.81	0.78 (0.89)	134	35.0 (35.7)	1.14 (1.09)	6.1 (6.1)	0.0157	0.033	0.060
Pins 1	0.0090	6.75	0.86 (0.92)	64	31.4 (34.0)	1.55 (1.29)	3.3 (3.4)	0.0278	0.012	0.042
Wood-Rich Pool-Riffle										
Pins 2	0.0133	6.90	0.61 (0.66)	70	36.0 (39.5)	0.96 (0.92)	7.8 (7.2)	0.0580	0.026	0.112
Flu hardy	0.0105	6.64	0.53 (0.55)	69.5	24.4 (29.1)	0.89 (0.85)	5.2 (2.6)	0.0455	0.044	0.118
Mill	0.0143	8.41	0.83 (1.04)	73	19.4 (24.0)	0.98 (0.87)	4.8 (4.1)	0.1450	0.048	0.120
Dry 1§	0.0222	7.96	0.60 (0.73)	70	53.4 (55.4)	0.96 (0.91)	10.8 (10.8)	0.0431	0.029	0.079
Skunk 1	0.0040	13.39	0.78 (0.85)	140	19.8 (23.8)	0.95 (0.86)	4.9 (2.2)	0.0352	0.030	0.072
Cedar	0.0046	10.95	0.72 (0.85)	100	27.2 (29.7)	0.72 (0.72)	5.9 (9.5)	0.0438	0.037	0.085

S (center-line bed slope), W (bank-full channel width), h (cross sectionally averaged bank-full channel depth), D_{50} (median bed-surface grain size), σ_g (graphic standard deviation [*Folk*, 1974]), LWD per square meter (total wood loading, pieces per square meter), $(\alpha/\lambda)_b$ (bar amplitude/wavelength), and $(\alpha/\lambda)_w$ (streamwise bank topography, amplitude/wavelength, one side of channel) are reach-average values. L is reach length. SE_{50} is the standard error of the reach-average D_{50} (see text).

*First values are cross sectionally averaged over the channel bed and banks, while those in parentheses are averaged over the channel bed only. We use the latter for calculating the bank-full depth-slope product in equation (5).

†Values in parentheses are for grain-size distributions with suspendable sizes removed (see text).

‡Here σ_g is the graphic standard deviation, defined as $(\phi_{84} - \phi_{16})/2$ [*Folk*, 1974], where ϕ_{84} and ϕ_{16} are the $\log_2$ grain sizes [*Krumbein*, 1936] for which 16% and 84%, respectively, of the surface grain sizes are finer.

§Evidence of ancient, catastrophic sediment inputs from debris flows.

‖Evidence of recent debris-flow inputs.

¶Bed load and suspended load material could not be differentiated as the maximum suspendable grain size was <2 mm, the minimum resolution used for our surface pebble counts.

chutes and slope failures. The geology of southeastern Alaska is characterized by all major rock types of ages ranging from Proterozoic(?) to Quaternary [*Gehrels and Berg*, 1992], largely accreted during the Cretaceous to Eocene [*Goldfarb et al*., 1988; *Gehrels et al*., 1990]. Southeastern Alaska was profoundly influenced by Pleistocene glaciation [*Reed*, 1958], and many channels drain glacially carved valleys and cirques. The Alaskan study sites include both pristine old growth environments and areas heavily disturbed by timber harvesting. Pristine channels were characterized by high wood loading, while disturbed channels were generally clear-cut to the stream banks and had most or all of their in-channel wood removed [*Wood-Smith and Buffington*, 1996]. Channel widths and slopes of our study sites ranged from 5 to 29 m and from 0.0017 to 0.0267, respectively (Table 1).

At each Alaskan study site, five cross sections and a center-line bed profile were surveyed with an engineer's level over reaches that were 8 to 23 channel widths long. A bank-to-bank random pebble count [*Wolman*, 1954] of 100^+ grains was conducted at each cross section, with grains smaller than 2 mm grouped as a single category. Reach-average grain-size statistics were determined from simple averages of these samples, with the suspendable load removed as described in section 3.1. Suspendable grain sizes ranged from 1 to 9 mm.

3.3. Wood Loading

The study sites exhibit a continuum of wood loading that strongly influences pool spacing (Figure 2). We used the median value of this continuum (0.03 pieces/m^2) to divide the channels into wood-poor and wood-rich categories.

4. Results

4.1. Reach-Scale Response

Our field data demonstrate that for a given reach-average, total bank-full shear stress ($\tau_{0_{bf}}$), channels with greater roughness (and therefore lower τ'_{bf} (equation (2)) have systematically smaller reach-average surface grain sizes (Figure 3). The progressive increase in bank, bar, and wood roughness causes a corresponding reduction in reach-average D_{50} at our study sites. This result is consistent with several other studies that demonstrate that wood removal from forest channels causes bed-surface coarsening, presumably because of increased bed shear stress resulting from loss of wood roughness (see review by *Lisle* [1995]). The solid line in Figure 3 is the low-roughness prediction of competence (see (5), $\tau^*_{c50} = 0.03$). As expected, the data show that surface grain sizes approach the theoretical competence curve at low hydraulic roughness (plane-bed morphology), as τ'_{bf} approaches $\tau_{0_{bf}}$.

There is considerable variability in the magnitude of textural fining caused by bank, bar, and wood roughness (Figure 4). Although the distributions of textural response overlap, the central tendencies of textural fining (25th–75th percentiles) are distinct for each channel type (Figure 4). The ratio of observed-to-predicted D_{50} has a median value of 0.53 for plane-bed channels, 0.30 for wood-poor pool-riffle channels, and 0.18 for wood-rich pool-riffle channels; this represents a reduction of roughly 40% from one channel type to the next. In channels with significant hydraulic roughness (wood-rich pool-riffle channels), observed D_{50} can be up to 90% less than the predicted competent value for the bank-full stage.

Table 1b. Reach-Average Alaskan Channel Characteristics

Channel	S	W, m	h,* m	L, m	D_{50},† mm	$\sigma_g(\phi)$†,‡	SE_{50},† mm	LWD Per Square Meter	$(\alpha/\lambda)_b$	$(\alpha/\lambda)_w$
Plane-Bed/Incipient Pool-Riffle										
Maybeso 3	0.0024	27.07	1.03 (1.11)	324	36.4 (39.6)	>1.50 (1.17)	2.1 (2.8)	0.0132	0.007	0.021
Maybeso 4	0.0036	24.48	1.06 (1.12)	436	46.4 (47.7)	0.88 (0.82)	4.1 (3.9)	0.0058	0.004	0.020
Indian	0.0122	24.60	1.17 (1.32)	480	79.4 (85.1)	1.67 (1.54)	10.0 (9.3)	0.0025	0.014	0.054
Weasel‖	0.0025	15.10	0.92 (1.01)	187	25.6 (48.2)	>2.34 (1.45)	8.8 (6.0)	0.0230	0.014	
Wood-Poor Pool-Riffle										
12 Mile 1	0.0021	23.34	0.95 (1.05)	360	24.3 (26.6)	1.44 (0.89)	2.6 (2.1)	0.0106	0.010	0.045
12 Mile 2	0.0028	22.47	1.03 (1.10)	170	21.9 (24.9)	1.90 (0.90)	3.2 (3.0)	0.0108	0.016	0.040
Maybeso 1	0.0095	22.31	1.13 (1.24)	400	49.6 (53.2)	1.76 (1.51)	5.1 (5.6)	0.0000	0.015	
Maybeso 2	0.0065	29.12	0.97 (1.10)	500	36.2 (38.6)	1.30 (1.16)	4.3 (4.2)	0.0112	0.013	
Cable	0.0017	16.89	0.88 (0.96)	300	20.6¶	>1.97¶	6.4¶	0.0234	0.023	0.083
FUBAR 1	0.0106	17.84	0.62 (0.66)	360	42.9 (47.5)	>1.50 (1.15)	9.2 (7.7)	0.0290	0.012	0.071
FUBAR 2	0.0127	16.32	0.79 (0.85)	300	57.6 (60.8)	1.58 (1.41)	4.5 (4.4)	0.0070	0.014	0.024
Muri	0.0150	14.29	0.59 (0.64)	300	44.3 (53.5)	>2.13 (1.29)	5.2 (4.3)	0.0123	0.015	0.060
Bambi	0.0102	4.6	0.32	80	16.3 (17.7)	>1.08 (0.85)	2.0 (1.7)	0.0136	0.025	0.075
Wood-Rich Pool-Riffle										
Hook§	0.0110	21.37	0.82 (0.88)	250	27.4 (31.9)	>1.78 (1.07)	2.1 (1.6)	0.0405	0.040	0.100
Trap 1	0.0055	12.92	0.84 (0.95)	165	17.0 (17.8)	1.04 (0.97)	3.0 (2.8)	0.0644	0.040	
Trap 2	0.0074	15.59	0.66 (0.77)	220	15.4 (16.0)	1.30 (1.11)	1.7 (1.4)	0.0635	0.037	
Trap 3	0.0072	11.84	0.60 (0.66)	220	13.9 (16.5)	>1.72 (1.21)	1.7 (0.7)	0.0639	0.045	
Trap 4	0.0071	9.67	0.68 (0.76)	220	13.5 (16.2)	>1.83 (1.34)	1.1 (0.8)	0.0698	0.032	
Trap 5	0.0102	14.11	0.68 (0.75)	175	17.6 (21.2)	>1.54 (0.98)	1.4 (1.1)	0.0591	0.048	
Trap 6	0.0120	15.76	0.71 (0.78)	200	13.4 (18.7)	>1.88 (1.10)	1.5 (2.3)	0.0566	0.038	
E Fk Trap 1	0.0133	15.72	0.78 (0.87)	200	19.9 (23.5)	>1.84 (1.00)	1.4 (1.3)		0.038	
E Fk Trap 2	0.0127	10.65	0.58 (0.66)	172	24.5 (31.0)	1.79 (1.20)	3.9 (1.9)	0.0531	0.051	
Fowler 1	0.0063	18.03	0.65 (0.74)	225	14.1 (18.5)	>2.03 (1.55)	3.6 (3.6)	0.0313	0.023	0.058
Fowler 2	0.0054	11.46	0.68 (0.83)	210	19.0 (24.5)	>2.06 (1.57)	7.6 (9.5)	0.0358	0.034	0.048
Fish 1	0.0267	19.18	1.12 (1.33)	167	30.6 (40.9)	1.32 (0.90)	4.0 (3.3)	0.0601	0.052	0.126
Fish 2	0.0224	12.88	0.56 (0.60)	280	45.8 (48.3)	1.33 (1.23)	2.5 (2.4)	0.0311	0.034	0.077
Greens‖	0.0220	12.90	0.66 (0.85)	260	34.9 (47.0)	>2.16 (1.58)	6.8 (5.7)	0.0303	0.039	0.055

See Table 1a for explanatory footnotes.

4.2. Roughness Configuration and Magnitude

The scatter of D_{50} values in Figure 3 for a given $\tau_{0_{bf}}$ and channel type reflects site-specific differences in roughness configuration. For example, wood creates hydraulic roughness primarily through form drag, the magnitude of which depends on the frequency, size, orientation, and height above the bed of the in-channel logs and rootwads. Similarly, the form drag caused by bars depends on their amplitude and wavelength [*Nelson and Smith*, 1989]. Several sources contribute to what we collectively call bank roughness: (1) proximity of channel banks (so-called width-to-depth effects) and associated momentum diffusion [*Leighly*, 1932; *Parker*, 1978]; (2) roughness length scale (i.e., skin friction) of the material forming the banks [*Einstein*, 1934, 1942; *Houjou et al*., 1990]; (3) downstream variations in channel width that effectively force lateral form drag analogous to bed form drag; and (4) riparian vegetation protruding from the banks and causing additional form drag.

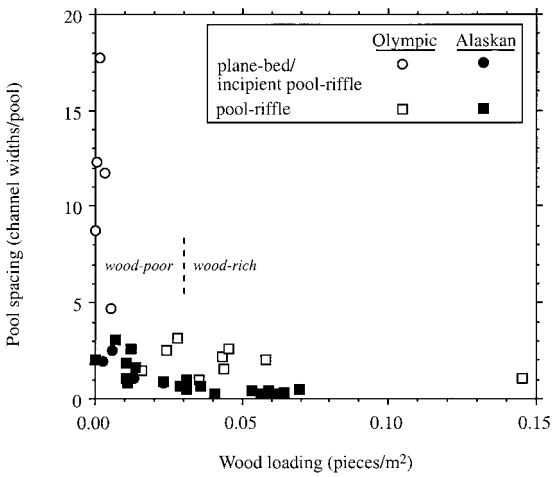

Figure 2. Pool spacing as a function of wood loading. Pool spacing is expressed in channel widths per pool, defined as (L/W)/number of pools, where L is reach length and W is bank-full width. Wood loading is defined as number of pieces/(WL). Although the ordinate and abcissa contain common factors, the observed relationship is not spurious [*Buffington*, 1998].

The physical channel characteristics that cause bank, bar, and wood roughness show a statistically significant increase in magnitude across the three channel types studied (Figure 5). For example, while there is no significant difference in width-to-depth ratios (W/h) amongst the channels (Figure 5a and Table 2), there is a significant increase in streamwise bank topography and consequent form drag (Figure 5b and Table 2). Streamwise variation of channel width at the study sites results in undulating banks and lateral form drag, the magnitude of which depends on the amplitude-wavelength ratio of the bank undulations ($(\alpha/\lambda)_w$, a reach-average value for each side of the channel). This ratio increases significantly across the three channel types (Figure 5b and Table 2), indicating a progressive increase in hydraulic roughness because of greater bank form drag.

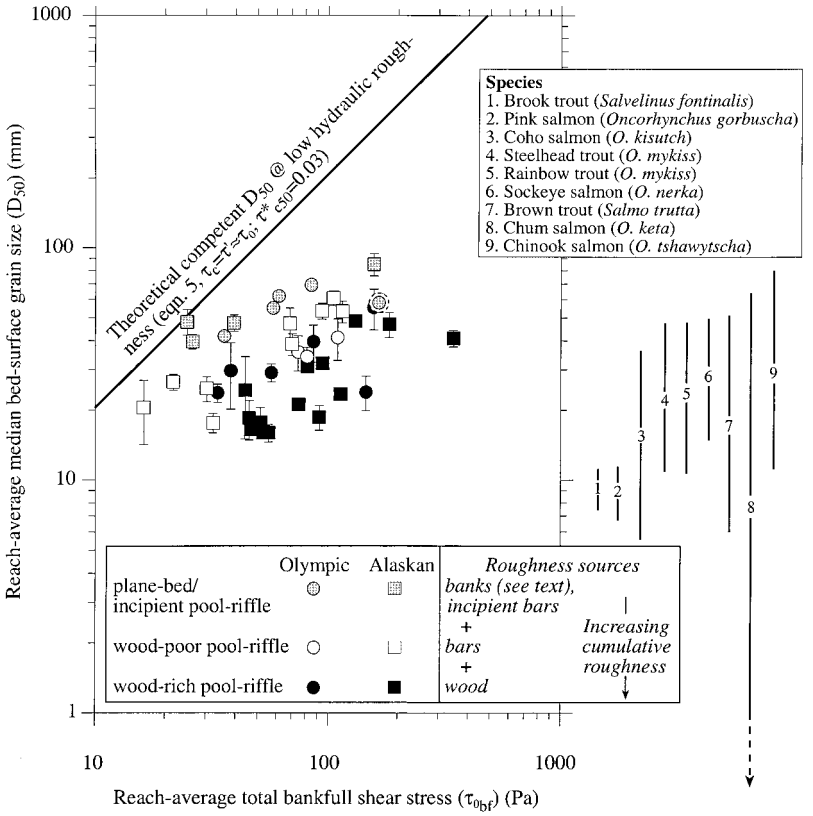

Figure 3. Median bed-surface grain size versus total bank-full boundary shear stress stratified by channel type. The solid line is the low-roughness prediction of competent D_{50} as a function of $\tau_{0_{bf}}$ (equation (5), $\tau^*_{c50} = 0.03$). Circled point is a plane-bed channel recently impacted by sediment input from a debris flow. Error bars represent the standard error; where not shown, the error is smaller than the symbol size (Table 1). Also shown are ranges of D_{50} values preferred by spawning salmonids [*Kondolf and Wolman*, 1993], the significance of which is discussed later in the paper. The reported ranges of spawning gravels likely contain considerable error and may be biased toward small sizes because (1) stream beds typically were sampled using the approach of *McNeil and Ahnell* [1960] which combines surface an subsurface material and (2) in some cases the coarse tails of the size distribution were arbitrarily truncated [*Kondolf and Wolman*, 1993].

Differences in bank skin friction and protrusion of riparian vegetation into the channel were not quantified. However, the greatest amount of vegetative protrusion into the channel typically occurred at the wood-poor pool-riffle sites where growth of riparian shrubs and deciduous trees was stimulated by recent clear-cutting.

Like streamwise bank topography, the amplitude-wavelength ratio of bars ($(\alpha/\lambda)_b$) shows a statistically significant increase across the three channel types (Figure 5c and Table 2), indicating a progressive increase in roughness due to bed form drag. Two scales of bars are included in Figure 5c: macroscale bars ($\alpha_b > 0.5\ h$) and mesoscale bars ($0.25\ h < \alpha_b < 0.5\ h$). Bar forms were identified visually from detrended bed profiles.

There is also a significant increase in wood loading across the three channel types (Figure 5d and Table 2), resulting in a progressive increase in hydraulic roughness due to wood form drag. Wood loading plays an important morphologic and hydrologic role at the study sites, not only influencing pool spacing (Figure 2) but also controlling the amplitude-wavelength ratio of both bank and bed topography (Figure 6). Forest channels commonly exhibit considerable width variation within a single reach [*Trimble*, 1997] because of morphologic forcing caused by in-channel wood. Wood obstructions can force flow against banks, causing scour and the development of locally wide sections of channel, or they can armor banks and maintain locally narrow channel widths; both effects commonly occur within a single reach. While wood loading also influences

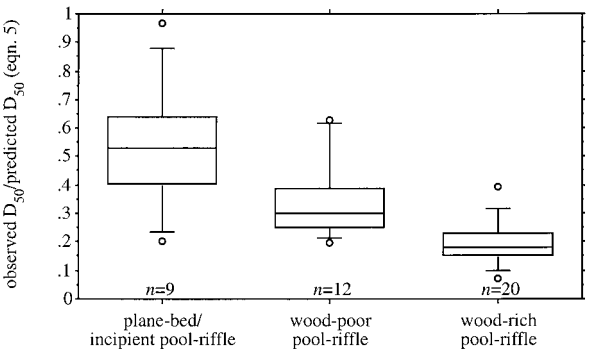

Figure 4. Box plots of textural fining defined as the ratio of observed-to-predicted D_{50}. Predicted values are calculated from equation (5). The line within each box is the median value of the distribution, box ends are the inner and outer quartiles, whiskers are the inner and outer tenths, and circles are the extrema. Variable n is the number of observations per distribution.

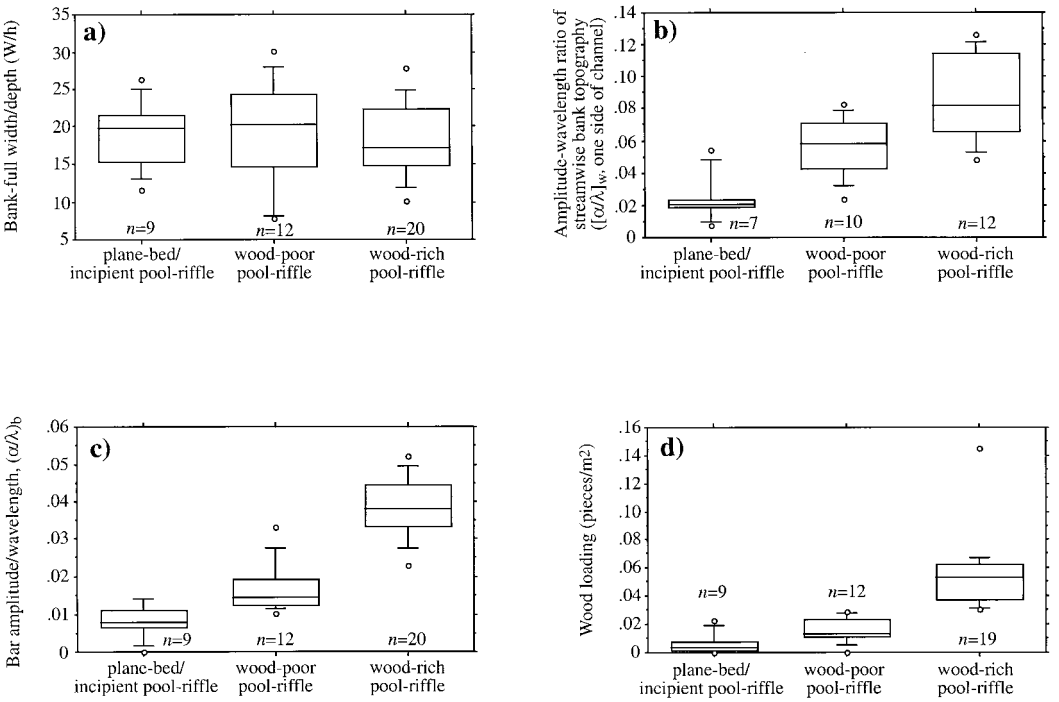

Figure 5. Box plots of reach-average (a) width-to-depth ratio, (b) amplitude-wavelength ratio of streamwise bank topography, (c) amplitude-wavelength ratio of bar topography, and (d) wood loading. See Figure 4 caption for box plot definition. Values used for these plots are listed in Table 1.

bed topography (Figure 6b), we find that wood affects the spacing of bars more so than their amplitude (Figure 7). Our findings indicate that beyond creating its own form drag and hydraulic roughness, wood forces greater bank and bed topography and consequently greater form drag at our study sites.

4.3. Subreach-Scale Response

Detailed field measurements at the Olympic sites allow examination of subreach-scale textural response to hydraulic roughness. Representative maps of each channel type illustrate characteristic variations in topography, wood loading, and surface texture (Figure 8). The number of textural types observed in a reach varied from one to seven, with textures composed of grain sizes ranging from silt to small boulders (Table 3). Two-sample median tests (a nonparametric kind of t test [*Conover*, 1971]) indicate that almost all textural types within a reach are significantly different from one another ($P \leq 0.05$), while most patches of the same textural type within a reach are statistically similar ($P > 0.05$).

Facies mapping demonstrates that channel type and roughness configuration strongly influence the number, frequency, and spatial arrangement of surface textures. Plane-bed channels exhibit one to four grain-size facies but are frequently monotextural (Table 3). Each of the wood-poor pool-riffle channels are composed of four textural types, while wood-rich pool-riffle channels exhibit three to seven facies types per reach (Table 3). Similarly, the total number of textural patches within a reach ranges from 1 to 8 in plane-bed channels but increases to 13–24 in wood-poor pool-riffle channels and 17–55 in wood-rich pool-riffle streams (Table 3). Furthermore, the spatial arrangement of textures is progressively more complicated in the three channel types studied (Figure 8).

Textural patches likely represent spatial divergence of sediment supply and transport capacity, causing local, size-selective variations in sediment flux that lead to patch development. Our field observations suggest that increased frequency and magnitude of flow obstructions (i.e., bars and wood) enhance the spatial divergence of sediment flux and patch development. For example, the number of textural patches in a reach is related to the frequency of wood obstructions (Figure 9). Although the stochastic nature of wood re-

Table 2. Comparison of Roughness Characteristics Between Channel Types

	P Values			
	W/h	$(\alpha/\lambda)_w$	$(\alpha/\lambda)_b$	Wood Pieces Per Square Meter
Plane-bed versus wood-poor pool-riffle	0.801	0.024	0.044	0.044
Wood-poor pool-riffle versus wood-rich pool-riffle	0.465	0.029	<0.001	<0.001
Plane-bed versus wood-rich pool-riffle	0.599	0.002	0.001	<0.001

Reported P values are for two-sample median tests (a nonparametric sort of t test [*Conover*, 1971]) evaluated with a one-tailed χ^2 statistic. Differences between distribution means are considered statistically significant when $P \leq 0.05$.

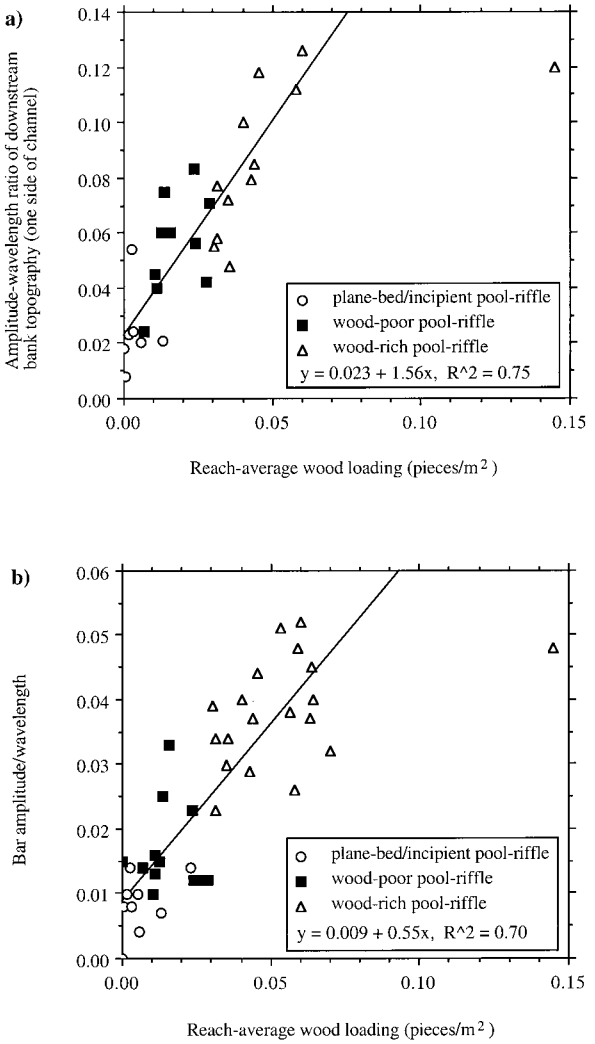

Figure 6. Reach-average amplitude-wavelength ratio of (a) bank topography and (b) bar topography as a function of wood loading. Mill Creek (far right triangle) is excluded from the curve fits.

cruitment creates complex, irregular textural patterns within our study sites, more predictable patterns of textural patches have been documented in channels with less chaotic arrangements of flow obstructions. For example, regular patterns of textural patches are found in self-formed meandering channels because of systematic downstream and cross-channel variations in shear stress and sediment flux caused by channel curvature, topographically induced convective accelerations, and lateral bed slope [*Dietrich et al*., 1979; *Dietrich and Smith*, 1984; *Parker and Andrews*, 1985].

Paired surface and subsurface sampling of textural patches demonstrates a strong correlation between surface and subsurface median grain sizes (Figure 10). Coarser textural patches have correspondingly coarser subsurface sizes [see also *Buffington and Montgomery*, 1999]. Moreover, we observe little to no armoring at our sites. We find that ratios of surface-to-subsurface D_{50} are within the typically observed range of 1–3 [*Milhous*, 1973; *Bathurst*, 1987; *Kinerson*, 1990; *Pitlick and Van Streeter*, 1998] but tend to cluster near 1 for our study sites, indicating poorly armored surfaces. Hydraulic roughness and reduced τ' likely inhibit armor development in these channels.

5. Discussion

Our results demonstrate that reach-average D_{50} is systematically finer in channels with greater hydraulic roughness. However, the overall trend of the data in Figure 4 has a somewhat lower slope than the reference D_{50} prediction (equation (5)). This apparent disagreement between theory and observation may be due to the small size of our data set. For example, data from gravel-bed rivers in Colorado [*Andrews*, 1984] support the grain-size prediction quite well (Figure 11a); the data trend with the prediction, and the limit of competence in these channels is well-described by the prediction. These data also support our hypothesis regarding textural response to hydraulic roughness, demonstrating that channels with thicker riparian vegetation (and therefore greater hydraulic resistance offered by the banks) have relatively smaller bed-surface grain sizes. Thicker riparian vegetation also increases bank strength, promoting smaller width-depth ratios that may reduce both bed shear stress and surface grain size. Data from gravel-bed rivers in the United Kingdom [*Hey and Thorne*, 1986] also trend with the grain-size prediction which, again, forms a good upper envelope of channel competence (Figure 11b).

It is important to note, however, that only gravel-bed channels with plane-bed morphologies (definition of *Montgomery and Buffington* [1997]) have the potential to realize the predicted reference values of D_{50}. Both lower-gradient sand-bed rivers and steeper-gradient boulder-bed rivers have characteristic channel morphologies and accompanying roughness elements that cause $\tau' \ll \tau_0$, and therefore observed values of

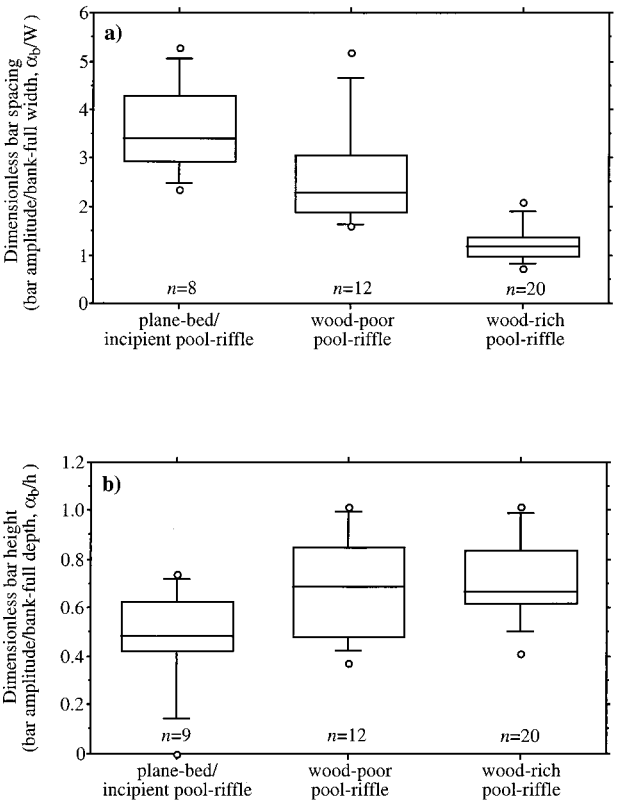

Figure 7. Box plots of reach-average, dimensionless bar wavelength and amplitude. See Figure 4 caption for box plot definition.

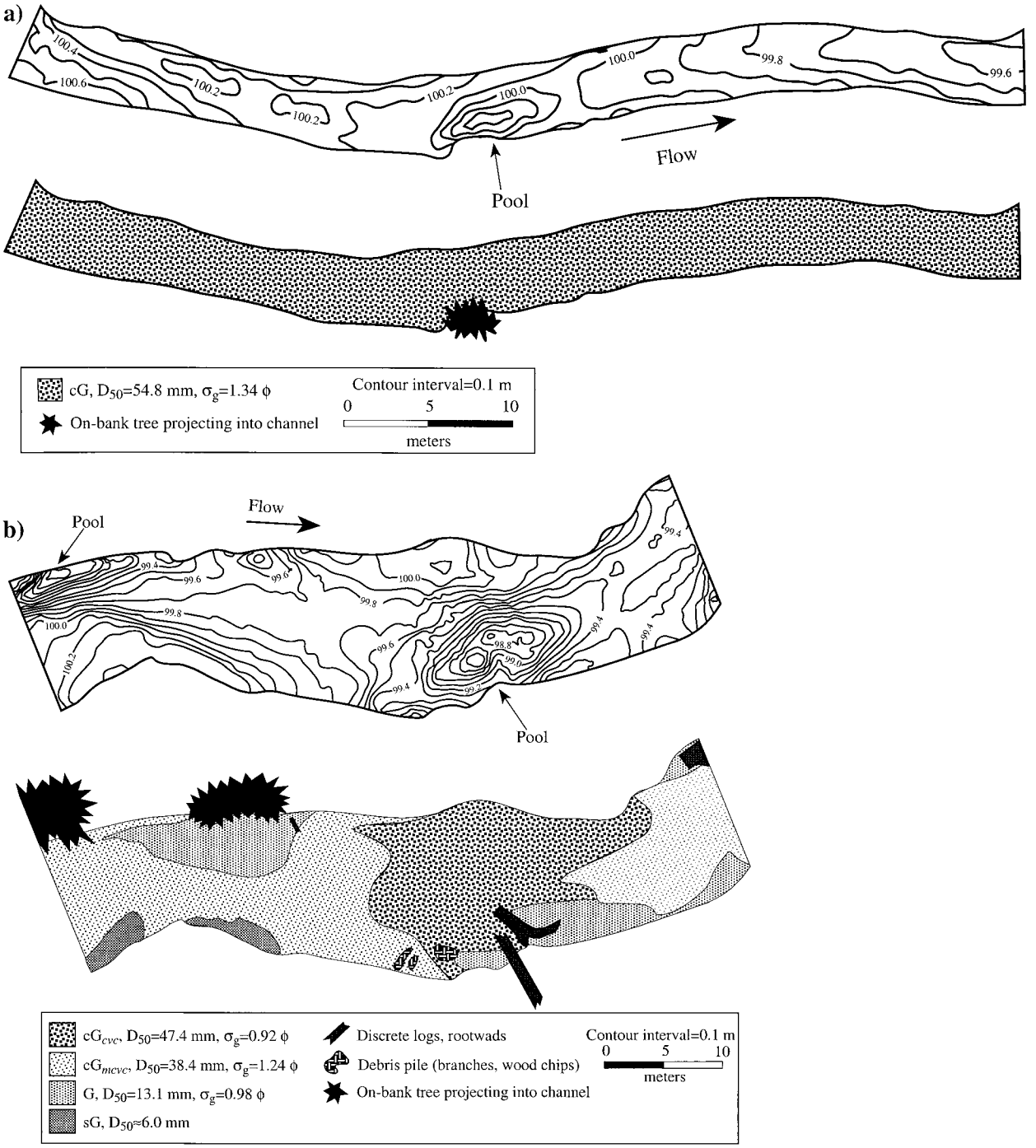

Figure 8. Morphologic and textural plan maps of typical (a) plane-bed (Hoko River 2), (b) wood-poor pool-riffle (Hoko River 1), and (c) wood-rich pool-riffle (Mill Creek) channels studied on the Olympic Peninsula [from *Buffington and Montgomery*, 1999]. See Table 3 for texture definitions. Boundary between channel bed and walls defines the lateral margin of the maps.

D_{50} much less than those predicted from (5) (Figure 12). Sand-bed rivers typically have a dune-ripple morphology characterized by multiple scales of bed forms (ripples, dunes, and bars) that provide significant form drag, while steeper-gradient boulder-bed channels typically have step-pool and cascade morphologies characterized by tumbling flow, low width-to-depth ratios, and boulder form drag, all of which create considerable channel roughness [*Montgomery and Buffington*, 1997]. Dune-ripple channels also exhibit sediment transport at stages significantly less than bank-full, indicating that the observed D_{50} should be much less than a theoretical competent D_{50} predicted from bank-full shear stress.

Even when limited to gravel-bed morphologies (i.e., plane-bed and pool-riffle channels), (5) overpredicts the competent D_{50} in channels with steep slopes because of unaccounted-for effects of particle form drag. As grain size becomes a significant proportion of the flow depth, it creates form drag that diminishes τ' and the competent D_{50}, an effect that is not

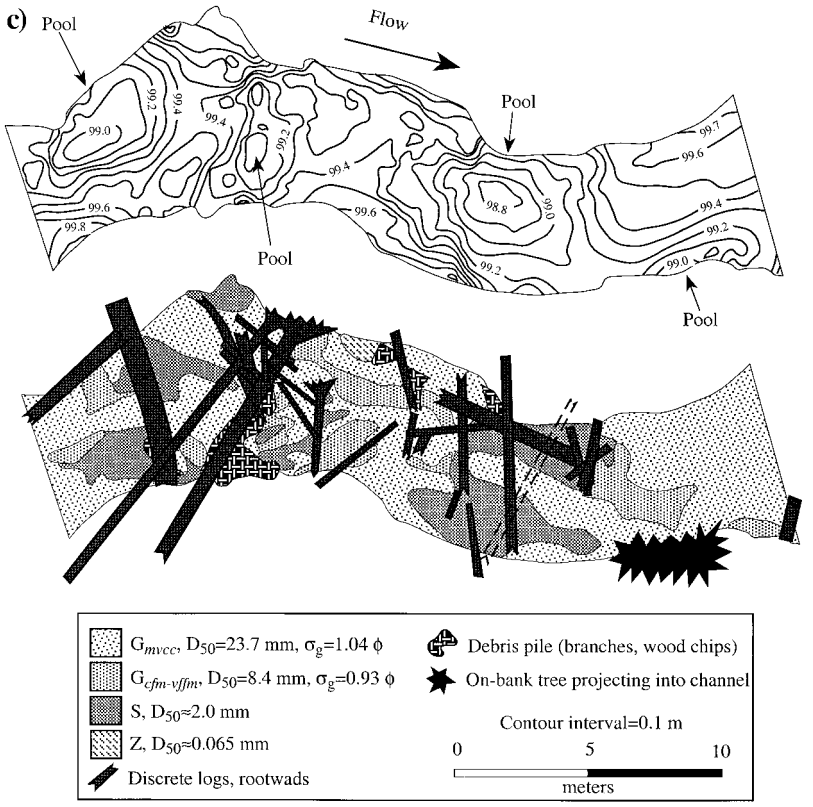

Figure 8c. (continued)

accounted for in (5). Particle form drag is represented by the relative roughness ratio (D_{50}/h). For given values of ρ, ρ_s, and τ^*_{c50}, (5) specifies a unique value of D_{50s}/h for each value of S

$$D_{50}/h = S \Big/ \left[\tau^*_{c50} \left(\frac{\rho_s}{\rho} - 1 \right) \right] \tag{6}$$

Consequently, large particle form drag is predicted for channels with steep slopes. Channel slope ranged from 0.0017 to 0.027 at our study sites, corresponding with values of D_{50}/h equal to 0.03–0.5 (equation (6)) and a 2–32% overprediction of competent D_{50} because of unaccounted-for effects of grain form drag [*Buffington*, 1998]. However, more than 80% of our study sites had slopes <0.015, indicating less than 17% overprediction of competence for the majority of our data.

Because our reported values of D_{50} are reach averages, it is important to examine whether the standard error of these average values exceeds the inferred textural response to hydraulic roughness thus influencing our interpretation of the data. The standard error of the reach-average D_{50} is defined as

$$\mathrm{SE}_{50} = s_{50}/\sqrt{n} \tag{7}$$

For the Washington channels, s_{50} is the standard deviation of median grain sizes of textures weighted by their area, and n is the number of textural types per reach. For the Alaskan channels, s_{50} is the standard deviation of median grain sizes of the channel-spanning pebble counts, and n is the number of pebble counts per reach. We find that the standard errors are substantial at some sites, but the pattern of decreasing grain size with increasing roughness due to banks, bars, and wood is maintained and is not obscured by the standard errors (Figure 3). For the most part the standard errors are small because even in very patchy reaches there is typically a dominant textural type that occupies ≥50% of the bed-surface area (Table 3), which skews the distribution of textural types and resultant reach-average D_{50} toward the grain size characteristics of the dominant textural type.

Because we did not quantify either the rate or caliber of sediment supply at the field sites, one may wonder if the textural fining observed in Figures 3 and 4 is due to systematic changes in either of these factors, rather than a systematic increase in hydraulic roughness and lowered τ'. In particular, laboratory studies demonstrate that bed-surface grain size varies inversely with sediment supply rate [*Buffington and Montgomery*, this issue]. However, it is unlikely that the textural fining observed here represents either an underlying increase in sediment supply rate or a decrease in supply caliber for several reasons. (1) The highest sediment loading is expected for sites in logged basins, where high sediment production rates occur because of two factors: fluvial erosion and mass wasting caused by poor road design [*Montgomery*, 1994; *Best et al*., 1995] and hillslope failures caused by reduced root strength following timber harvest [*Sidle et al*., 1985]. However, the logged sites (predominantly wood-poor pool-riffle sites) do not show the highest degree of textural fining (Figure 3). The channels with the greatest amount of textural fining (wood-rich pool-riffle channels) are predominantly roadless old growth sites with a lower frequency of mass wasting events. Therefore the observed textural fining is not due to an increasing sediment supply rate. (2) Lithology (a strong control on grain strength and caliber) is highly variable across the sites and is uncorrelated with the three channel types. (3) Drainage area (a

Table 3. Surface Texture Composition of the Olympic Channels

Channel	Texture*	Percentage of Bed	Frequency (Number/Reach)	D_{50},† mm	$\sigma_g(\phi)$†,‡
			Plane-Bed/Incipient Pool-Riffle		
Dry 2	gC	100	1	67.1 (69.2)	1.24 (1.17)
Alder	G	0.4	1	~11	
	scG	9.0	4	21.8 (29.7)	1.76 (1.39)
	cG	90.6	1	56.1 (61.0)	1.58 (1.27)
Hoko 2	cG	100	1	54.8 (55.2)	1.34 (1.31)
Hoh 1	S	2	2	~2.0 (NA)	
	cgS	63	3	9.0 (42.7)	2.76 (1.26)
	cG	35	3	38.9 (40.3)	1.10 (1.05)
Hoh 2	S	4	2	~2.0 (NA)	
	cgS	4	1	9.0 (42.7)	2.76 (1.26)
	cG	0.5	1	38.9 (40.3)	1.10 (1.05)
	gC	91.5	1	61.4 (63.1)	1.54 (1.49)
			Wood-Poor Pool-Riffle		
Skunk 2	S	9.33	9	<2.0 (8.5)	>0.65 (0.40)
	G	11.19	9	9.9 (12.8)	1.41 (1.05)
	csG	8.22	4	25.0 (27.8)	1.37 (0.98)
	cG	71.24	2	50.4 (51.5)	1.10 (1.05)
Hoko 1	sG	5.10	7	~6.0	
	G	13.87	9	13.1 (13.8)	0.98 (0.87)
	cG_{mcvc}	61.58	4	38.4 (39.2)	1.24 (1.20)
	cG_{cvc}	19.45	3	47.4 (47.7)	0.92 (0.92)
Pins 1	S	1.16	3	~2.0 (NA)	
	G_{cfm}	4.15	6	9.2 (11.0)	1.32 (1.02)
	$G_{fcm-fmc}$	2.58	3	12.7 (14.1)	1.15 (1.04)
	cG	92.11	1	33.3 (35.6)	1.57 (1.31)
			Wood-Rich Pool-Riffle		
Pins 2	S	7.71	4	~2.0 (NA)	
	sG	3.22	3	7.1 (8.7)	0.92 (0.47)
	cG_{mvcc}	48.47	3	29.6 (30.4)	0.93 (0.88)
	cG_{mcvc}	40.61	7	52.4 (52.8)	1.01 (1.00)
Flu Hardy	Z	3.98	2	~0.06 (NA)	
	S	11.79	9	~2.0 (NA)	
	G_{cfm}	3.70	6	11.7 (12.0)	0.92 (0.90)
	G_{mcvc}	80.53	1	29.5 (29.9)	0.89 (0.85)
Mill	Z	1.63	2	~0.06 (NA)	
	S	15.89	21	~2.0 (NA)	
	$G_{cfm-vffm}$	11.77	25	8.4 (10.4)	0.93 (0.67)
	G_{mvcc}	62.57	2	23.7 (24.5)	1.04 (0.94)
	G_{cvc}	8.15	5	39.6 (39.6)	0.58 (0.58)
Dry 1	S	0.94	3	~2.0 (NA)	
	scG	4.79	2	9.3 (33.9)	2.34 (1.90)
	G	7.52	5	13.8 (15.7)	1.09 (0.87)
	cG	39.28	3	39.1 (39.6)	1.12 (1.09)
	gC	47.48	8	77.0 (77.0)	0.66 (0.66)
Skunk 1	S	16.15	32	~2.0 (NA)	
	G_{vcmc}	62.31	6	21.2 (22.0)	0.96 (0.84)
	G_{mvcc}	21.54	4	29.2 (29.2)	0.91 (0.91)
Cedar	Z	5.61	2	~0.06 (NA)	
	S	2.64	3	~2.0 (NA)	
	sG	1.08	6	6.6 (7.2)	0.98 (0.84)
	G_{vcmc}	12.80	11	17.6 (17.6)	0.65 (0.65)
	G_{mvcc}	64.19	1	26.6 (26.8)	0.70 (0.70)
	cG	6.15	1	35.3 (35.3)	0.82 (0.82)
	gC	7.53	3	74.4 (74.4)	0.89 (0.89)

*Textures are named using the *Buffington and Montgomery* [1999] classification scheme. Capital letters represent the dominant grain size (Z, silt; S, sand; G, gravel; and C, cobble), preceding lower case letters represent less abundant grain sizes, read as adjectives modifying the upper case noun (s, sandy; g, gravelly; and c, cobbley), and succeeding lower case subscripts further describe the grain size composition of the dominant size class (*vf*, very fine; *f*, fine; *m*, medium; *c*, coarse; and *vc*, very coarse). Order of lower case letters indicates relative abundance (least to greatest). For example, sG_{fm} is sandy, fine to medium gravel. Lower case subscripts are used to distinguish otherwise identical textural names (e.g., distinguishing coarse versus fine gravel textures). Sediment terms correspond with standard grain size classes [*Buffington and Montgomery*, 1999, Table 1]. NA indicates the entire suspension of a patch at bank-full flow.

†Values in parentheses are are for grain-size distributions with suspendable sizes removed (see text).

‡Here σ_g is the graphic standard deviation, defined as $(\phi_{84} - \phi_{16})/2$ [*Folk*, 1974], where ϕ_{84} and ϕ_{16} are the $\log_2$ grain sizes [*Krumbein*, 1936] for which 16% and 84%, respectively, of the surface grain sizes are finer.

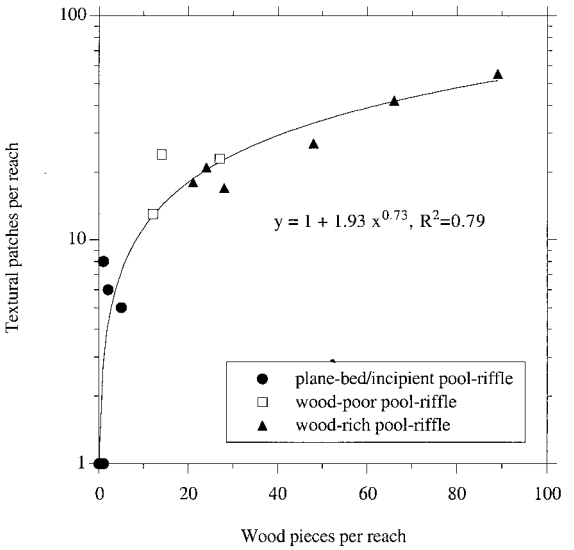

Figure 9. Textural patch frequency as a function of wood frequency at the Olympic study sites. The fitted curve is forced to one patch in plane-bed reaches with zero pieces of wood.

crude surrogate for sediment supply rate and caliber) is uncorrelated with channel type.

The strong grain size response to hydraulic roughness (Figure 3), and the lack of evidence for an underlying covariance with sediment supply that would explain the observed textural fining, suggests that site-specific differences in sediment supply rate and caliber are overwhelmed by bank, bar, and wood roughness at our study sites, except where recent catastrophic sediment inputs have occurred. For example, one of the plane-bed study sites recently impacted by a debris flow has a reach-average median grain size considerably finer than the other plane-bed channels (circled point in Figure 3), presumably in response to catastrophic sediment loading of the debris flow. Infrequent, catastrophic sediment inputs from hollow failures and resultant debris flows are characteristic of the steep, mountainous terrain of northwestern Washington and southeastern Alaska. Evidence for such impacts observed at our field sites include (1) landslide tracks entering a channel, in some cases accompanied by a debris jam, and (2) fresh debris flow levees, with inundated and scoured riparian vegetation. Although six of our study sites showed evidence of debris-flow input (Table 1), only one of the most recently affected channels showed a strong textural response to debris-flow loading.

A more detailed study of the influence of hydraulic roughness on reach-average bed-surface grain size was conducted at one of our wood-poor pool-riffle channels and one of our wood-rich pool-riffle channels [*Buffington*, 1998]. Bed shear stresses for these sites were calculated from a theoretical stress-partitioning model that was verified through a course of field study. Results show that observed reach-average values of D_{50} are within 1–10% of those predicted from the bank-full bed stress. These findings indicate that bed-surface grain sizes at those sites are in quasi-equilibrium with bank-full channel hydraulics and suggest that hydraulic roughness, rather than sediment supply, is the dominant control on grain size.

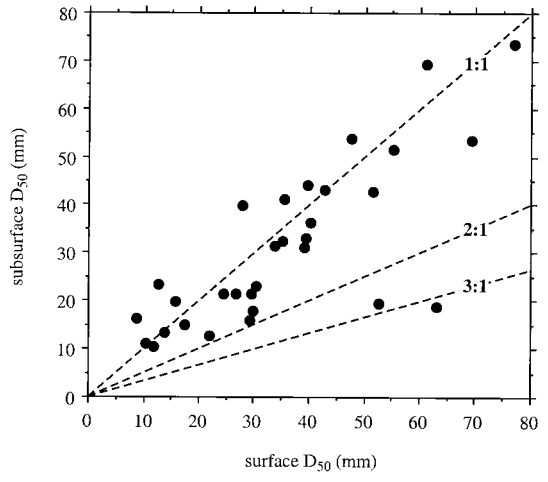

Figure 10. Surface median grain size versus subsurface value for textural patches sampled at the Olympic study sites. Particle sizes that are suspendable at bank-full stage were removed from both grain-size distributions (see section 3). Subsurface grain-size distributions were determined from sieved bulk samples, following the *Church et al.* [1987] sampling criterion (i.e., the largest grain is ≤1% of the total sample weight).

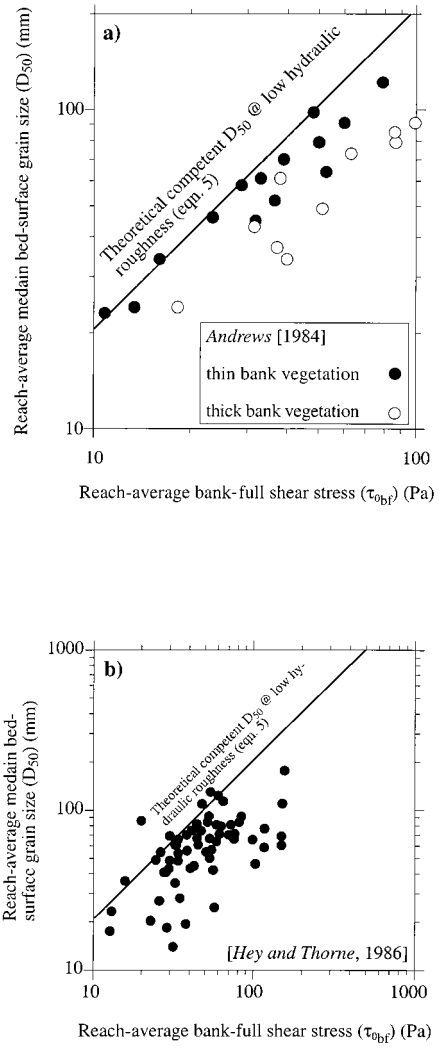

Figure 11. Median bed-surface grain size versus total bank-full shear stress for gravel-bed channels in (a) Colorado [*Andrews*, 1984] and (b) the United Kingdom [*Hey and Thorne*, 1986]. Solid line is that of Figure 3.

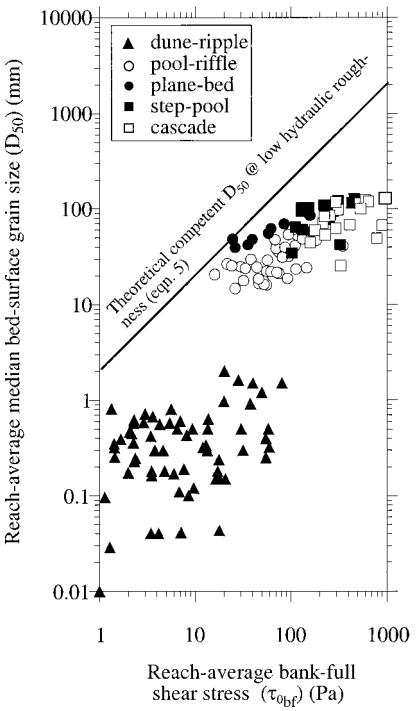

Figure 12. Median bed-surface grain size versus total bank-full shear stress, stratified by reach morphology (definitions of *Montgomery and Buffington* [1997]). Data sources are as follows: dune-ripple [*Simons and Albertson*, 1963; *Chitale*, 1970; *Higginson and Johnston*; 1988]; plane-bed and pool-riffle [*Lisle*, 1989; *Lisle and Madej*, 1992; this study]; and step-pool and cascade [*Montgomery and Buffington*, 1997]. Solid line is that of Figure 3.

Textural fining caused by hydraulic roughness also has important implications for the availability of salmonid spawning habitat. Salmonids select specific grain sizes in which to spawn [*Kondolf and Wolman*, 1993]. Comparison of preferred spawning-gravel sizes and our field data suggest that textural fining caused by banks, bars, and wood can create usable spawning gravels in channels otherwise too coarse to be hospitable for spawning (Figure 3). Furthermore, bar and wood roughness create a greater variety of textural patches (see Figures 8a–8c), offering a range of aquatic habitats that may promote biologic diversity or be of use to specific animals at different life stages. Macroinvertebrates also exhibit grain-size preferences when selecting aquatic habitat [*Cummins and Lauff*, 1969; *Reice*, 1980].

Our approach for predicting a low-roughness reference D_{50} uses a reach-average depth-slope product to approximate the total boundary shear stress. This approximation assumes steady, uniform flow at reach scales. These conditions are satisfied when discharge fluctuations occur on timescales $\gg u/gS$ and when study reach lengths are $\gg h/S$ [*Paola and Mohrig*, 1996]. Although our study sites are characterized by high velocities (~1 m/s at bank-full stage) and flashy hydrographs, the steep channel slopes ($\sim 10^{-3}$–10^{-2}) make u/gS quite small (<2 min) and considerably less than the timescale for significant discharge variations during flood events (rising limb of hydrograph is typically ≥5 hours [*Estep and Beschta*, 1985; *Smith et al*., 1993]). Consequently, a quasi-steady flow approximation is valid for our study sites. However, the ratio of study reach length to h/S ranges from 0.4 to 10 (with an average of 3) and does not satisfy the criterion for quasi-uniform flow. Therefore a depth-slope product may only partially approximate the actual reach-average shear stress at each study site.

6. Conclusions

We find that surface grain sizes of gravel-bed rivers are responsive to hydraulic roughness caused by bank irregularities, bars, and wood debris. Progressive increases in hydraulic roughness cause systematic textural fining, presumably because of lowered bed stresses which, in turn, reduce channel competence and diminish bed load transport capacity, both of which promote textural fining. In hydraulically rough forest channels the observed reach-average D_{50} can be as low as one tenth the competent value predicted from the total bank-full boundary shear stress. This suggests a corresponding difference between the bed shear stress and the total boundary shear stress for bed surfaces that are in equilibrium with channel hydraulics and highlights the importance of accounting for hydraulic roughness in complex alluvial channels. Because many bed load transport equations are power functions of the difference between the applied and critical shear stresses, small errors in the bed stress can cause large errors in calculated bed load transport rates.

We also find that at subreach scales our study channels are composed of discrete textural patches that vary with channel morphology and roughness configuration. Previous studies demonstrate that textural patches also develop and evolve in response to altered sediment load in plane-bed and pool-riffle channels [*Dietrich et al*., 1989; *Lisle et al*., 1993]. Despite the common occurrence of textural patches in both natural [*Dietrich and Smith*, 1984; *Ferguson et al*., 1989; *Kinerson*, 1990; *Wolcott and Church*, 1990; *Lisle and Madej*, 1992; *Paola and Seal*, 1995; *Powell and Ashworth*, 1995] and laboratory channels [*Iseya and Ikeda*, 1987; *Dietrich et al*., 1989; *Lisle et al*., 1993], little is known about the processes and mechanics of patch development, patch interactions, and their role in bed load transport and channel stability.

The analysis framework presented here provides a theoretical reference point for examining textural response to hydraulic roughness. However, surface grain size also is responsive to bed load sediment supply [*Buffington and Montgomery*, this issue]. Consequently, it may be difficult to assess relative causes for textural fining when channels have both high sediment loading and significant hydraulic roughness. To isolate the effects of sediment supply, a method for partitioning channel shear stress is required, such that the competent median grain size can be calculated from the bed shear stress (τ') rather than the total boundary shear stress (τ_0) [*Buffington and Montgomery*, this issue]. Moreover, use of surface grain size to assess magnitudes of hydraulic roughness and bed load sediment supply require channels to be in quasi-equilibrium. Surface textures that have not had sufficient time to equilibrate with channel hydraulics and imposed sediment loads may not be good indicators of these quantities. Nevertheless, our approach provides a physically based framework for examining controls on bed-surface grain size. With the above caveats in mind our framework can be used as a starting point for interpreting physical processes and assessing channel condition based on inspection of bed-surface grain size.

Acknowledgments. Financial support was provided by the Washington State Timber, Fish and Wildlife agreement (TFW-SH10-FY93-

004 and FY95-156) and the Pacific Northwest Research Station of the USDA Forest Service (cooperative agreement PNW 94-0617). ITT Rayonier Corporation graciously provided access to their land on the Olympic Peninsula. We thank Mike Church, Rob Ferguson, John Pitlick, Jim Pizzuto, Peter Wilcock, and an anonymous reviewer for insightful criticisms of earlier drafts of this work.

References

Andrews, E. D., Bed-material entrainment and hydraulic geometry of gravel-bed rivers in Colorado, *Geol. Soc. Am. Bull*., *95*, 371–378, 1984.

Bathurst, J. C., Measuring and modeling bedload transport in channels with coarse bed materials, in *River Channels: Environment and Process*, edited by K. S. Richards, pp. 272–294, Blackwell, Cambridge, Mass., 1987.

Best, D. W., H. M. Kelsey, D. K. Hagans, and M. Alpert, Role of fluvial hillslope erosion and road construction in the sediment budget of Garrett Creek, Humboldt County, California, *U.S. Geol. Surv. Prof. Pap*., *1454-M*, 9 pp., 1995.

Buffington, J. M., The use of streambed texture to interpret physical and biological conditions at watershed, reach, and subreach scales, Ph.D. dissertation, 147 pp., Univ. of Wash., Seattle, 1998.

Buffington, J. M., and D. R. Montgomery, A systematic analysis of eight decades of incipient motion studies, with special reference to gravel-bedded rivers, *Water Resour. Res*., *33*, 1993–2029, 1997.

Buffington, J. M., and D. R. Montgomery, A procedure for classifying textural facies in gravel-bed rivers, *Water Resour. Res*., *35*, 1903–1914, 1999.

Buffington, J. M., and D. R. Montgomery, Effects of sediment supply on surface textures of gravel-bed rivers, *Water Resour. Res*., this issue.

Buffington, J. M., W. E. Dietrich, and J. W. Kirchner, Friction angle measurements on a naturally formed gravel streambed: Implications for critical boundary shear stress, *Water Resour. Res*., *28*, 411–425, 1992.

Carling, P., The concept of dominant discharge applied to two gravel-bed streams in relation to channel stability thresholds, *Earth Surf. Processes Landforms*, *13*, 355–367, 1988.

Carling, P. A., and M. A. Hurley, A time-varying stochastic model of the frequency and magnitude of bed load transport events in two small trout streams, in *Sediment Transport in Gravel-Bed Rivers*, edited by C. R. Thorne, J. C. Bathurst, and R. D. Hey, pp. 897–920, John Wiley, New York, 1987.

Chien, N., The present status of research on sediment transport, *Trans. Am. Soc. Civ. Eng*., *121*, 833–884, 1956.

Chitale, S. V., River channel patterns, *J. Hydraul. Div. Am. Soc. Civ. Eng*., *96*, 201–221, 1970.

Church, M. A., D. G. McLean, and J. F. Wolcott, River bed gravels: Sampling and analysis, in *Sediment Transport in Gravel-Bed Rivers*, edited by C. R. Thorne, J. C. Bathurst, and R. D. Hey, pp. 43–88, John Wiley, New York, 1987.

Conover, W. J., *Practical Nonparametric Statistics*, 462 pp., John Wiley, New York, 1971.

Cummins, K. W., and G. H. Lauff, The influence of substrate particle size on the microdistribution of stream macrobenthos, *Hydrobiologia*, *34*, 145–181, 1969.

Dietrich, W. E., Settling velocity of natural particles, *Water Resour. Res*., *18*, 1615–1626, 1982.

Dietrich, W. E., and J. D. Smith, Bed load transport in a river meander, *Water Resour. Res*., *20*, 1355–1380, 1984.

Dietrich, W. E., J. D. Smith, and T. Dunne, Flow and sediment transport in a sand bedded meander, *J. Geol*., *87*, 305–315, 1979.

Dietrich, W. E., J. D. Smith, and T. Dunne, Boundary shear stress, sediment transport and bed morphology in a sand-bedded river meander during high and low flow, in *River Meandering*, *Proceedings of the Conference Rivers '83*, edited by C. M. Elliot, pp. 632–639, Am. Soc. of Civ. Eng., New York, 1984.

Dietrich, W. E., J. W. Kirchner, H. Ikeda, and F. Iseya, Sediment supply and the development of the coarse surface layer in gravel-bedded rivers, *Nature*, *340*, 215–217, 1989.

Dietrich, W. E., M. E. Power, K. O. Sullivan, and D. R. Montgomery, The use of an analytical reference state in watershed analysis, *Geol. Soc. Am. Abstr. Programs*, *28*, 62, 1996.

du Boys, P., Le Rhône et les rivièrs a lit affouillable, *Ann. Ponts Chaussées*, *Mem. Doc*., *5*, *18*, 141–195, 1879.

Einstein, A., Der hydraulische oder profil-radius, *Schweiz. Bauztg*., *103*, 89–91, 1934.

Einstein, H. A., Formulas for the transportation of bed load, *Trans. Am. Soc. Civ. Eng*., *107*, 561–597, 1942.

Einstein, H. A., and R. B. Banks, Fluid resistance of composite roughness, *Eos Trans. AGU*, *31*, 603–610, 1950.

Einstein, H. A., and N. L. Barbarossa, River channel roughness, *Trans. Am. Soc. Civ. Eng*., *117*, 1121–1146, 1952.

Estep, M. A., and R. L. Beschta, Transport of bedload sediment and channel morphology of a southeast Alaska stream, *For. Serv. Res. Note PNW-430*, 15 pp., U.S. Dep. of Agric., Portland, Oreg., 1985.

Ferguson, R. I., K. L. Prestegaard, and P. J. Ashworth, Influence of sand on hydraulics and gravel transport in a braided gravel bed river, *Water Resour. Res*., *25*, 635–643, 1989.

Folk, R. L., *Petrology of Sedimentary Rocks*, 182 pp., Hemphill, Austin, Tex., 1974.

Gehrels, G. E., and H. C. Berg, Geologic map of southeastern Alaska, *U.S. Geol. Surv. Misc. Invest. Ser*., *I-1867*, 1992.

Gehrels, G. E., W. C. McClelland, S. D. Samson, P. J. Patchett, and J. L. Jackson, Ancient continental margin assemblage in the northern Coast Mountains, southeast Alaska and northwest Canada, *Geology*, *18*, 208–211, 1990.

Goldfarb, R. J., D. L. Leach, W. J. Pickthorn, and C. J. Paterson, Origin of lode-gold deposits of the Juneau gold belt, southeastern Alaska, *Geology*, *16*, 440–443, 1988.

Henderson, F. M., Stability of alluvial channels, *Trans. Am. Soc. Civ. Eng*., *128*, 657–720, 1963.

Hey, R. D., Bar form resistance in gravel-bed rivers, *J. Hydrol. Eng*., *114*, 1498–1508, 1988.

Hey, R. D., and C. R. Thorne, Stable channels with mobile gravel beds, *J. Hydraul. Eng*., *112*, 671–689, 1986.

Higginson, N. N. J., and H. T. Johnston, Estimation of friction factor in natural streams, in *International Conference on River Regime*, edited by W. R. White, pp. 251–266, John Wiley, New York, 1988.

Houjou, K., Y. Shimizu, and C. Ishii, Calculation of boundary shear stress in open channel flow, *J. Hydrosci. Hydraul. Eng*., *8*, 21–37, 1990.

Howard, A. D., Thresholds in river regimes, in *Thresholds in Geomorphology*, edited by D. R. Coates and J. D. Vitek, pp. 227–258, Allen and Unwin, Winchester, Mass., 1980.

Iseya, F., and H. Ikeda, Pulsations in bedload transport rates induced by a longitudinal sediment sorting: A flume study using sand and gravel mixtures, *Geogr. Ann*., *69A*, 15–27, 1987.

Johnston, C. E., E. D. Andrews, and J. Pitlick, In situ determination of particle friction angles of fluvial gravels, *Water Resour. Res*., *34*, 2017–2030, 1998.

Kellerhals, R., and D. I. Bray, Sampling procedures for coarse fluvial sediments, *J. Hydraul. Div. Am. Soc. Civ. Eng*., *97*, 1165–1180, 1971.

Kinerson, D., Bed surface response to sediment supply, M.S. thesis, 420 pp., Univ. of Calif., Berkeley, 1990.

Kirchner, J. W., W. E. Dietrich, F. Iseya, and H. Ikeda, The variability of critical shear stress, friction angle, and grain protrusion in water worked sediments, *Sedimentology*, *37*, 647–672, 1990.

Kondolf, G. M., and M. G. Wolman, The sizes of salmonid spawning gravels, *Water Resour. Res*., *29*, 2275–2285, 1993.

Krumbein, W. C., Application of logarithmic moments to size frequency distributions of sediments, *J. Sediment. Petrol*., *6*, 35–47, 1936.

Leighly, J. B., Toward a theory of the morphologic significance of turbulence in the flow of water in streams, *Univ. Calif. Publ. Geogr*., *6*, 1–22, 1932.

Leopold, L. B., M. G. Wolman, and J. P. Miller, *Fluvial Processes in Geomorphology*, 522 pp., W. H. Freeman, New York, 1964.

Li, R., D. B. Simons, and M. A. Stevens, Morphology of cobble streams in small watersheds, *J. Hydraul. Div. Am. Soc. Civ. Eng*., *102*, 1101–1117, 1976.

Lisle, T. E., Sediment transport and resulting deposition in spawning gravels, north coastal California, *Water Resour. Res*., *25*, 1303–1319, 1989.

Lisle, T. E., Effects of coarse woody debris and its removal on a channel affected by the 1980 eruption of Mount St. Helens, Washington, *Water Resour. Res*., *31*, 1797–1808, 1995.

Lisle, T. E., and M. A. Madej, Spatial variation in armouring in a channel with high sediment supply, in *Dynamics of Gravel-Bed Rivers*, edited by P. Billi et al., pp. 277–293, John Wiley, New York, 1992.

Lisle, T. E., F. Iseya, and H. Ikeda, Response of a channel with alternate bars to a decrease in supply of mixed-size bed load: A flume experiment, *Water Resour. Res.*, *29*, 3623–3629, 1993.

McNeil, W. J., and W. H. Ahnell, Measurement of gravel composition of salmon stream beds, *Circ. 120*, 2 pp., Fish. Res. Inst., Coll. of Fish., Univ. of Wash., Seattle, 1960.

Meyer-Peter, E., and R. Müller, Formulas for bed-load transport, in *Proceedings of the 2nd Meeting of the International Association for Hydraulic Structures Research*, pp. 39–64, Int. Assoc. for Hydraul. Res., Delft, Netherlands, 1948.

Milhous, R. T., Sediment transport in a gravel-bottomed stream, Ph.D. dissertation, 232 pp., Ore. State Univ., Corvallis, 1973.

Montgomery, D. R., Road surface drainage, channel initiation, and slope instability, *Water Resour. Res.*, *30*, 1925–1932, 1994.

Montgomery, D. R., and J. M. Buffington, Channel-reach morphology in mountain drainage basins, *Geol. Soc. Am. Bull.*, *109*, 596–611, 1997.

Naot, D., Response of channel flow to roughness heterogeneity, *J. Hydraul. Eng.*, *110*, 1568–1587, 1984.

Nelson, J. M., and J. D. Smith, Flow in meandering channels with natural topography, in *River Meandering*, *Water Resour. Monogr.*, vol. 12, edited by S. Ikeda and G. Parker, pp. 69–102, AGU, Washington, D. C., 1989.

O'Brien, M. P., and B. D. Rindlaub, The transportation of bed-load by streams, *Eos Trans. AGU*, *15*, 593–603, 1934.

Paola, C., and D. Mohrig, Paleohydraulics revisited: Palaeoslope estimation in coarse-grained braided rivers, *Basin Res.*, *8*, 243–254, 1996.

Paola, C., and R. Seal, Grain size patchiness as a cause of selective deposition and downstream fining, *Water Resour. Res.*, *31*, 1395–1407, 1995.

Parker, G., Self-formed straight rivers with equilibrium banks and mobile bed, 2, The gravel river, *J. Fluid Mech.*, *89*, 127–146, 1978.

Parker, G., Hydraulic geometry of active gravel rivers, *J. Hydraul. Div. Am. Soc. Civ. Eng.*, *105*, 1185–1201, 1979.

Parker, G., and E. D. Andrews, Sorting of bed load sediment by flow in meander bends, *Water Resour. Res.*, *21*, 1361–1373, 1985.

Parker, G., and P. C. Klingeman, On why gravel bed streams are paved, *Water Resour. Res.*, *18*, 1409–1423, 1982.

Parker, G., and A. W. Peterson, Bar resistance of gravel-bed streams, *J. Hydraul. Div. Am. Soc. Civ. Eng.*, *106*, 1559–1575, 1980.

Pitlick, J., and M. M. Van Streeter, Geomorphology and endangered fish habitats of the upper Colorado River, 1, Historic changes in streamflow, sediment load, and channel morphology, *Water Resour. Res.*, *34*, 287–302, 1998.

Powell, D. M., and P. J. Ashworth, Spatial pattern of flow competence and bed load transport in a divided gravel bed river, *Water Resour. Res.*, *31*, 741–752, 1995.

Prestegaard, K. L., Bar resistance in gravel bed steams at bankfull stage, *Water Resour. Res.*, *19*, 473–476, 1983.

Reed, J. C., Southeastern Alaska, in *Landscapes of Alaska*, edited by H. Williams, pp. 9–18, Univ. of Calif. Press, Berkeley, 1958.

Reice, S. R., The role of substratum in benthic macroinvertebrate microdistribution and litter decomposition in a woodland stream, *Ecology*, *61*, 580–590, 1980.

Shields, A., Anwendung der Aehnlichkeitsmechanik und der Turbulenzforschung auf die Geschiebebewegung, *Mitt. Preuss. Versuchsanst. Wasserbau Schiffbau*, *26*, 26 pp., 1936.

Sidle, R. C., A. J. Pearce, and C. L. O'Loughlin, *Hillslope Stability and Land Use*, *Water Resour. Monogr.*, vol. 11, 140 pp., AGU, Washington, D. C., 1985.

Simons, D. B., and M. L. Albertson, Uniform water conveyance channels in alluvial material, *Trans. Am. Soc. Civ. Eng.*, *128*, 65–167, 1963.

Smith, R. D., R. C. Sidle, and P. E. Porter, Effects on bedload transport of experimental removal of woody debris from a forest gravel-bed stream, *Earth Surf. Processes Landforms*, *18*, 455–468, 1993.

Tabor, R. W., and W. M. Cady, Geologic map of the Olympic Peninsula, Washington, *U.S. Geol. Surv. Misc. Invest. Ser.*, *I-994*, 1978a.

Tabor, R. W., and W. M. Cady, The structure of the Olympic Mountains, Washington: Analysis of a subduction zone, *U.S. Geol. Surv. Prof. Pap.*, *1033*, 38 pp., 1978b.

Trimble, S. W., Stream channel erosion and change resulting from riparian forests, *Geology*, *25*, 467–469, 1997.

Wathen, S. J., R. I. Ferguson, T. B. Hoey, and A. Werritty, Unequal mobility of gravel and sand in weakly bimodal river sediments, *Water Resour. Res.*, *31*, 2087–2096, 1995.

Wiberg, P. L., and J. D. Smith, Calculations of the critical shear stress for motion of uniform and heterogeneous sediments, *Water Resour. Res.*, *23*, 1471–1480, 1987.

Wiberg, P. L., and J. D. Smith, Velocity distribution and bed roughness in high-gradient streams, *Water Resour. Res.*, *27*, 825–838, 1991.

Wolcott, J., and M. Church, Strategies for sampling spatially heterogeneous phenomena: The example of river gravels, *J. Sediment. Petrol.*, *61*, 534–543, 1990.

Wolman, M. G., A method of sampling coarse bed material, *Eos Trans. AGU*, *35*, 951–956, 1954.

Wolman, M. G., and J. P. Miller, Magnitude and frequency of forces in geomorphic processes, *J. Geol.*, *68*, 54–74, 1960.

Wood-Smith, R. D., and J. M. Buffington, Multivariate geomorphic analysis of forest streams: Implications for assessment of land use impact on channel condition, *Earth Surf. Processes Landforms*, *21*, 377–393, 1996.

J. M. Buffington, Water Resources Division, U.S. Geological Survey, 3215 Marine Street, Building RL6, Boulder, CO 80303. (jbuffing@usgs.gov)

D. R. Montgomery, Department of Geological Sciences, University of Washington, Seattle, WA 98195. (dave@bigdirt.geology.washington.edu)

(Received July 27, 1998; revised April 21, 1999;
accepted April 23, 1999.)